ASSESSMENT OF STRESS CONCENTRATION ON DENTED PIPELINES

Bianca de Carvalho Pinheiro
COPPE/UFRJ, Ocean Engineering Dept., PO Box 68508
bianca@lts.coppe.ufrj.br

Ilson Paranhos Pasqualino
COPPE/UFRJ, Ocean Engineering Dept., PO Box 68508
ilson@lts.coppe.ufrj.br

Sérgio Barros da Cunha
TRANSPETRO/DT/GETEC
sbcunha@petrobras.com.br

Abstract. *A nonlinear finite element model was developed to assess stress concentration factors around different geometries of plain dents on pipelines. The numerical model comprised small strain plasticity and large rotations. Stress concentration factors were obtained by cycling the internal pressure within operational conditions. Experimental tests were carried out to determine the strain history of pipe models under denting simulation followed by cyclic internal pressure. The experimental results were used to validate the finite element model. Stress concentration factors for different geometries of API X60 grade steel dented pipes were obtained using the numerical model.*

Keywords*: Mechanical Damage, Plain Dents, Stress Concentration Factors, High Cycle Fatigue.*

1. Introduction

One of the possible failure modes of oil and gas pipelines is the high cycle fatigue due to stress concentration in dented sections. Cyclic loadings may be generated by fluid pressure and temperature changes and, in the case of marine risers, by the action of waves, wind and streams. This type of defect can be generated by the impact of an anchor, a rock, excavation equipment or any other heavy object. These defects may be of different types, like dents, excessive out of rounding, smooth localized buckles or wrinkles. The high cycle fatigue failure can produce leaks that may cause not only financial loss to the operator but also damage to the environment and population.

The pipeline fatigue failure associated with mechanical damage represents one of the causes of in service failures of oil and gas pipelines. Thus, the assurance of a safe pipeline operation is obtained with a consistent assessment of the mechanical damages. Moreover, the assessment of the structural integrity of pipes subjected to cyclic loads can avoid flow interruptions caused by unnecessary repairs or leaks. A great effort has been done to estimate stress concentration factors in damaged pipe sections through finite element models (Fowler, 1993 and Alexander and Kiefner, 1997) and some methods to assess the fatigue life of dented pipelines have been developed (Cosham and Hopkins, 2004), but there is still a lack of knowledge on this subject. The stress concentration factors are mainly function of the pipe and damage dimensions, the material properties and the boundary conditions. Based on the results of the early studies, it was concluded that some of these parameters may be further investigated.

This work initiated a study to assess the reduction in the estimated fatigue life due to stress concentration in dented pipes. The aim was the determination of stress concentration factors associated with plain dents defects caused by mechanical damage. With these stress concentration factors it becomes possible to calculate the estimated fatigue life through fatigue curves available in the literature. Until now, plain dents with a spherical shape have been the focus of the study.

A nonlinear three-dimensional finite element model was developed using shell elements to simulate local damage in the pipe and obtain stress concentration factors under cyclic internal pressure. The model was validated through experiments simulating the whole process. Small-scale pipe models were built and instrumented with electrical extensometers in order to obtain the strain history along denting simulation and, subsequently, the application of cyclic internal pressure. The numerical results of strain history were compared with those of the experiments to calibrate the FE model. Stress concentration factors for selected geometries of dented API X60 grade steel pipes were generated using the finite element model.

2. Experiments

The experimental study was developed within the workshop of the Submarine Technology Laboratory – COPPE/UFRJ. Small-scale models were manufactured in order to evaluate strain levels in dented steel pipes under internal pressure. The experiments comprise the simulation of initial damages in pipe models followed by the

application of internal pressure. The aim is to obtain the strain level evolution within the loading process. The experimental results are useful to understand the strain behavior and to validate the numerical model.

2.1. Small-scale models

The models were cut out from a steel pipe string with approximately 5 m length, 73 mm of external diameter (D) and 3.05 mm of wall thickness (t). Six small-scale models with total length (L) of 510 mm, approximately 7D, were machined. The average dimensions of the small-scale models are shown in Tab. 1.

Table 1. Average dimensions of the small-scale models.

Model	D (mm)	t (mm)	D/t	d/D (%)	x (mm)	θ (°)
23A	72.91	3.056	23.862	5	13.0	18.0
23C	73.01	3.041	24.008	5	13.0	18.0
23D	73.01	3.017	24.195	10	17.0	22.5
23E	73.01	3.049	23.947	10	17.0	22.5
23H	73.02	3.046	23.975	15	18.0	27.0
23I	73.03	3.059	23.875	15	18.0	27.0

Three test coupons were cut in the longitudinal direction of the pipe string (AISI 1020 grade steel) used to manufacture the small-scale models. They were tested in a conventional servo-hydraulic machine at a strain rate of approximately 10^{-4} s^{-1}. Strain gages were used to accurately evaluate the elastic material parameters. The average elasticity modulus, Poisson ratio and yield stress obtained are equal to 202213 N/mm^2, 0.299 and 272 N/mm^2, respectively.

The main purpose of the experiments is to acquire high levels of strain without compromising the physical integrity of the gage during the denting simulation. From the results of Tab. 1, the models were assumed to be 73.0 mm external diameter and 3.047 mm wall thickness, resulting in a D/t ratio of 23.96. These data and the material properties were used to run preliminary finite element analyses of denting simulation in order to determine the positions of the electrical extensometers (strain gages). Therefore, points of large strain levels around the dented region (pipe middle section) were determined for initial defects with d/D ratios of 5, 10 and 15%, where d is the radial depth of the dent. The sketch of Fig. 1 shows the instrumentation of the models using four biaxial strain gages, where the axial (x) and circumferential (θ) distances, according to the d/D ratio, are presented in Tab. 1. Figure 2 shows the instrumented model before the denting simulation.

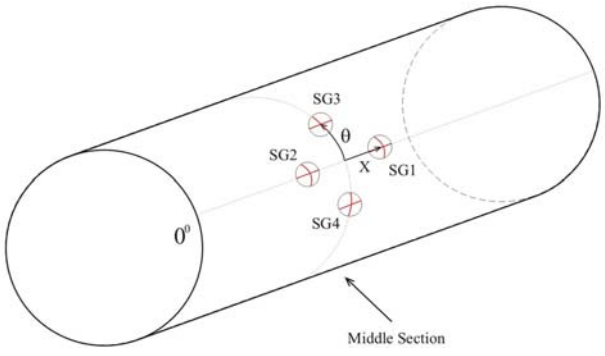

Figure 1. Position of the strain gages.

Figure 2. Small-scale model instrumentation.

2.2. Denting simulation

An experimental set up was developed to simulate initial damages on the small-scale models creating a localized region of stress concentration. It is comprised by a servo-hydraulic frame, with a 63.2 mm diameter cylindrical rod with a spherical tip, and a moving rigid table monitored by an electronic displacement transducer (Fig. 3). The model was carefully laid on the rigid table, so that the resultant dent could be centered in relation to the strain gages. The vertical displacement of the table is controlled by the servo hydraulic frame. The test signals of the strain gages, the displacement transducer and the LVDT frame are transferred to a data acquisition system connected to a PC.

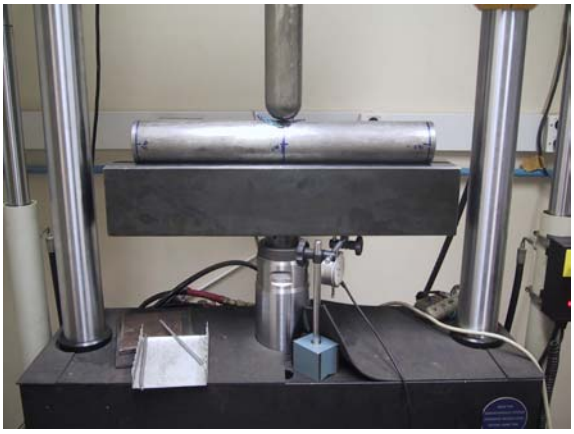

Figure 3. Experimental set up for denting simulation.

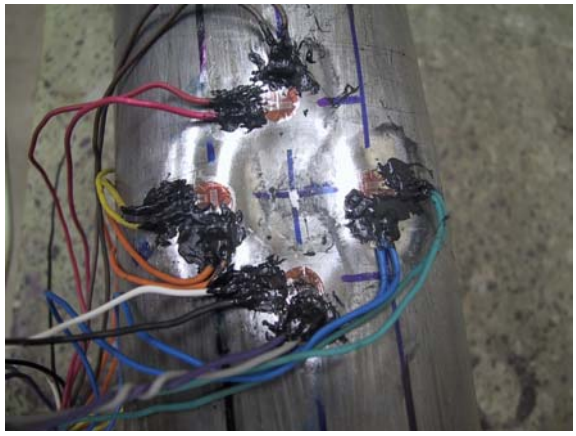

Figure 4. Small-scale model after being dented.

It can be verified in Fig. 4, showing the resulting dent in one model, that during indentation the die punches very near to the gages. Moreover, the strain levels obtained were even greater than 5%, what led in many cases to the detachment or loss of some gages. Obviously, placing gages far from the damaged region would prevent this inconvenience, but also would drive the measurements away from the area of higher strain levels. In view of this, it may be verified in Tab. 2 that the initial dents didn't coincide with the planned values, since the tests were conducted within the limits of the strain gages. Table 2 reports the maximum residual strains after the spring back of the structures, where the symbol (-) means a lost gage. In spite of the limitations of the adhesive used to fix the gages, strains of up to 7% were measured. Based on the position of the gages (Fig.1), it can be seen that the strains parallel to the perimeter of the dent are always compressive, while its count part are positive, in view of the Poisson effect.

Table 2. Results of residual strains around the dented region.

Model	*d/D* (%)	Residual Strains (%)							
		SG1		SG2		SG3		SG4	
		Hoop	Axial	Hoop	Axial	Hoop	Axial	Hoop	Axial
23A	4.22	-2.79	2.27	-2.68	2.27	1.48	-1.18	1.45	-1.61
23C	6.93	-5.14	3.38	-5.29	3.10	1.65	-2.34	2.03	-2.20
23D	10.03	-	-	-5.29	4.20	2.52	-2.42	-	-
23E	7.05	-3.44	3.08	-3.15	2.92	2.11	-1.81	2.20	-1.90
23H	9.62	-	-	-4.38	3.75	-	-	2.49	-2.33
23I	12.37	-7.02	4.70	-6.09	4.71	-	-2.39	-	-2.61

2.3. Internal pressure

The strain variation under internal pressure in the dented region of the small-scale models was investigated with the aid of an experimental set up (Fig. 5). It is composed of two end plugs with external grips that generate axial load under internal pressure. An electronic pressure transducer attached to one end plug monitors the pressure inside the pipe while a hydraulic pump operated by hand allows controlled pressurization of the model. The test signals of the strain gages and the pressure transducer are transferred to a data acquisition system.

The models 23C, 23D and 23I were selected to be tested under an internal pressure raging from 0 to 50% of MOP (maximum operating pressure). According to Alexander and Kiefner (1997), MOP corresponds to 72% of the specified minimum yield strength. Based on the estimated yield stress of 272 N/mm^2, it was defined an internal pressure ranging from 0 to 8.175 N/mm^2. As the applied internal pressure provides the "re-rounding" effect on the dented region of the pipe, i.e., the pipe wall undergoes further plastic strain, recovering partially its initial shape, the experiments were carried out in two steps. The pipe was pressurized from 0 to 8.175 N/mm^2 in each step. It can be verified in Fig. 6, for instance, where the accumulated strain is plotted versus the applied pressure, that the analyzed region works plastically at the first cycle and elastically at the second. It shows that dented steel pipes under cyclic internal pressure may be considered to deform elastically if the maximum internal pressure is kept unaltered. At the first cycle, the pipe undergoes the amount of re-rounding corresponding to the applied maximum pressure, but at the second, no more plastic strain will be accumulated, unless the maximum pressure is increased.

Figure 5. Experimental set up for internal pressure.

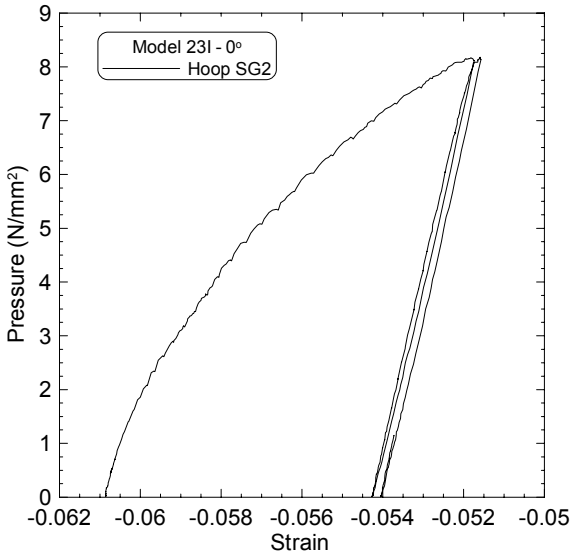

Figure 6. Experimental hoop strains of model 23I under internal pressure.

3. Numerical model

The numerical procedure was accomplished to determine stress concentration factors in dented pipes under internal pressure. A three-dimensional shell type elastic-plastic model was developed using the finite element method with the aid of the mainframe ABAQUS release 6.4 (ABAQUS, 2004). Through correlation between numerical and experimental results it was possible to evaluate the accuracy of the FEM developed.

3.1. Model geometry

The three basic components of the model are the pipe, the indenter and the saddle. The pipe is defined by the diameter of the middle surface (D_{ms}) and the wall thickness (t). A pipe longitudinal length of, approximately, 7D was adopted. This longitudinal length was selected in order to minimize any interaction between the dent area and the end of the pipe.

Analytical rigid surfaces were used to simulate the indenter and the saddle. The saddle supports the bottom portion of the pipe constraining its vertical displacements when the indenter is acting on the top portion. The radius of curvature of the saddle is larger than the pipe radius to prevent any over-constraining of the pipe bottom. The indenter had a spherical shape but others geometries can be easily generated for future analyses. The contact between the pipe and the rigid surfaces (indenter and saddle) was simulated with the aid of contact surfaces. The two areas of contact were the dent region between the pipe and the indenter and the bottom region, where contact with the saddle is expected.

3.2. Finite element mesh

Since shell elements are permitted whenever the diameter to thickness ratio is 20 or higher, solid continuum elements were not required in the analyses. Then, a three-dimensional shell model was developed employing the ABAQUS S8R5 second-order quadrilateral thin shell element, with five degrees of freedom per node (three translations and two surface rotations). This element type converges to thin shell theory as the thickness decreases (the Love-Kirchhoff hypothesis is satisfied numerically). The change in thickness with deformation is ignored in this element. And also, the S8R5 element type is automatically converted to the S9R5 type when a slave surface of a contact pair is associated to a region having S8R5 elements, because the die does not have a midface node, what can lead to convergence difficulties.

To minimize computational time in the numerical analyses, a quarter-symmetry model was used. There were adopted planes of symmetry in the longitudinal and transversal directions, planes 1-2 and 2-3, respectively, simplifying the model to 1/4 of the pipe geometry. The actual model length is then reduced to, approximately, *3.5D*.

The finite element model developed assumes large rotations (geometric nonlinearity), but admits only small deformations, according to the formulation of the element being used. The mesh is more refined at the dented region of the pipe and presents a smooth transition to a coarser mesh at the end of the pipe. The Fig. 7 shows the finite element mesh and the analytical surface that simulates the indenter.

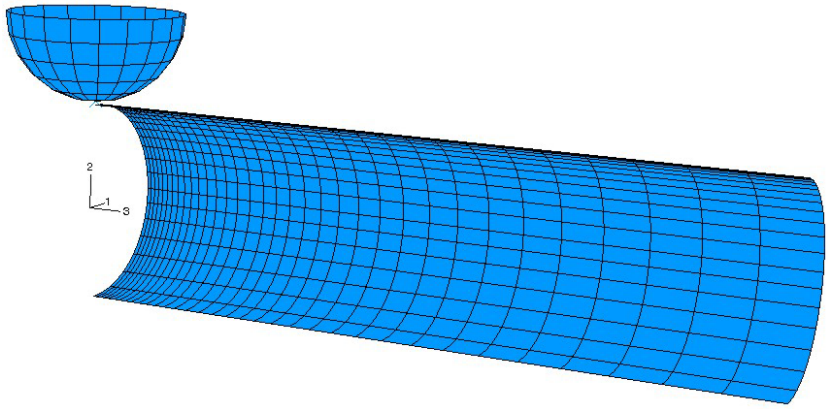

Figure 7. Finite element mesh and the indenter.

In order to accurately model the behavior of the pipe material in response to denting, spring back and cyclic pressurization, it was used a material model incorporating plasticity within the potential flow rule and the von Mises yield surface under combined isotropic and kinematic hardening. As the re-rounding effect (see 2.3) during the first cycle of pressurization confers reversed plastic deformation to the structure, the Bauschinger effect must be taken into account. Cyclic uniaxial tensile tests were not carried out, but an approximation provided by the ABAQUS routine, using only half cycle, can estimate this effect within the kinematic hardening theoretical approach. Values for the input of stress and strain data were determined through uniaxial tensile tests of the material adopted in the experimental tests. The average stress-strain curve was described using true stress and logarithmic plastic strains.

3.3. Boundary conditions and loading

The model simulated the following load steps: indentation to a depth specified as a percentage of the pipe diameter, removal of the indenter (spring back), and two cycles of internal pressure.

When the indenter is removed the pipe geometry remains partially deformed according to the intensity of the indentation and the level of plasticity attained. This final configuration retains residual stresses that perform a critical role in determining the alternating stresses induced in the cyclic internal pressure loading. The cyclic pressure range adopted is normally based upon of a percentage of MOP (see 2.3).

Three boundary conditions may be applied at the pipe edge: axially constrained, free, and closed edge (pressure vessel simulation). In the last case (pressure vessel), a force identical to that caused by an end cap is imposed. This load is applied by coupling the edge nodes with a reference node placed in the center of the pipe edge. The load is directly applied at the reference node and transmitted to the pipe edge.

4. Correlation between numerical and experimental results

In order to reproduce the experimental tests, the finite element model was generated using the material properties, boundary conditions and average dimensions of the small-scale models. The numerical results were compared with those obtained from the experimental tests. Initially, the results of the denting simulation were correlated with the residual strains and displacements of the numerical analyses (Tab. 3). Some observed discrepancies can be attributed to the positions of the strain gages, since the prescribed positions in Tab. 1 should not have been obtained precisely in practice. Additionally, small deviations from the planned position may cause significant differences in strain, since large strain gradients are observed in this region.

The strains observed during indentation of the models 23D and 23I are shown in Figs. 8 and 9. These graphs present the strain versus displacement of the die, comparing the numerical and experimental (gages SG3 and SG4) results. In general, the graphs showed good agreement between numerical and experimental strains. Finally, the strain behaviors under internal pressure in the numerical model and in the experiments were compared. The results are presented in Figs. 10 and 11. Unfortunately many of the gages were not preserved for the pressurization test, but the few results available proved that the numerical model can reproduce the experiments with good accuracy. In this case, the plasticity model assuming only isotropic hardening didn't give the strain response expected. The amount of strain occurred during re-rounding was only obtained when the combined isotropic and kinematic hardening was used.

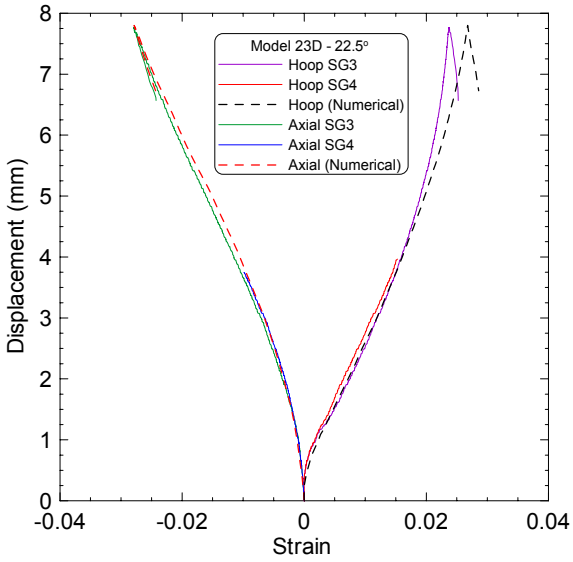

Figure 8. Numerical and experimental strains versus radial displacement of the die for the model 23D.

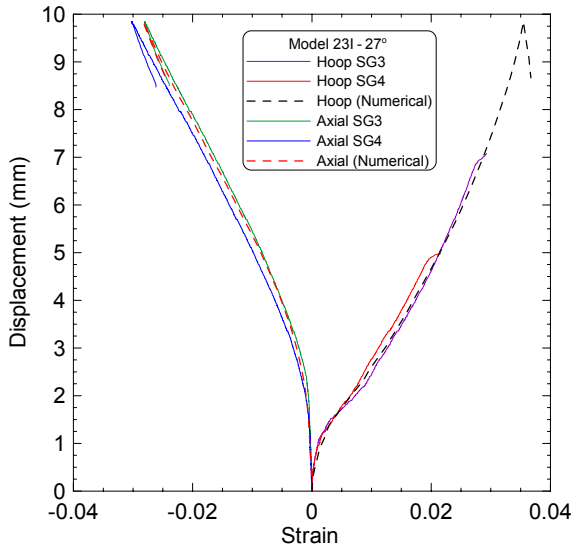

Figure 9. Numerical and experimental strains versus radial displacement of the die for the model 23I.

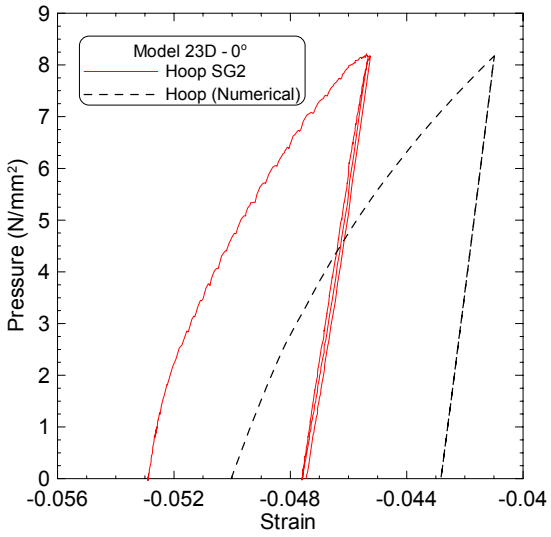

Figure 10. Numerical and experimental hoop strains versus internal pressure for the model 23 D.

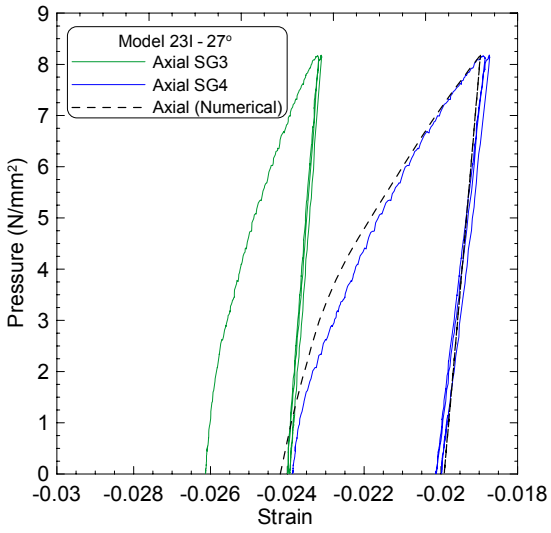

Figure 11. Numerical and experimental axial strains versus internal pressure for the model 23I.

Table 3. Numerical and experimental results of residual strains and displacements.

Model		*d/D* (%)	Residual Strains (%)							
			SG1 Hoop	SG2 Hoop	SG1 Axial	SG2 Axial	SG3 Hoop	SG4 Hoop	SG3 Axial	SG4 Axial
23A	Exp.	4.22	-2.79	-2.68	2.27	2.27	1.48	1.45	-1.18	-1.61
	Num.	4.00	-3.84		2.89		1.51		-1.52	
23C	Exp.	6.93	-5.14	-5.29	3.38	3.10	1.65	2.03	-2.34	-2.20
	Num.	6.60	-7.05		4.41		2.06		-2.62	
23D	Exp.	10.03	-	-5.29	-	4.20	2.52	-	-2.42	-
	Num.	9.23	-6.60		4.99		2.68		-2.79	
23E	Exp.	7.05	-3.44	-3.15	3.08	2.92	2.11	2.20	-1.81	-1.90
	Num.	6.60	-4.13		3.55		2.22		-1.89	
23H	Exp.	9.62	-	-4.38	-	3.75	-	2.49	-	-2.33
	Num.	9.23	-5.41		4.51		3.10		-2.01	
23I	Exp.	12.37	-7.02	-6.09	4.70	4.71	-	-	-2.39	-2.61
	Num.	11.88	-8.01		5.98		3.55		-2.83	

5. Determination of stress concentration factors (SCFs)

After the validation of the numerical model it was possible to determine stress concentration factors for different materials, geometries and boundary conditions of dented pipelines. In this case, the API X60 grade steel was selected. As the objective is not to reproduce the experimental tests, the boundary condition at the external edge was adopted as axial constrain. This condition seems to be more representative for infinite length pipes.

The geometric parameters adopted were a external diameter (D) equal to 12.75 in (323.85 mm) and wall thicknesses (t) that provide D/t ratios equal to 20, 30, 40, 50 and 60. The longitudinal length of the model was selected as, approximately, $2.5D$ (considering the symmetry condition). This length is considered sufficient to prevent any interaction between the dent area and the pipe edge. The indenter has a spherical shape with a diameter of 8.625 in (219.075 mm).

The model has the following load steps: indentation, removal of the indenter, followed by to steps of internal pressure. The cyclic pressure varies from 0 to 50% MOP, where MOP is function of the model geometry, since it depends on the D/t ratio. The value of MOP varied from 25.814 to 8.60472 N/mm^2 for the D/t ratio ranging from 20 to 60, respectively.

The stress concentration factor (K_t) is calculated using the definition:

$$K_t = \Delta\sigma_{max} / \Delta\sigma_{nom} \tag{1}$$

where $\Delta\sigma_{max}$ is the maximum variation of hoop stress, considering all elements of the finite element mesh, between the load steps of minimum and maximum internal pressure and $\Delta\sigma_{nom}$ is the variation of the nominal hoop stress corresponding to the internal pressure range. The nominal hoop stress in thin walled circular cylindrical shells under internal pressure (p) is given by:

$$\sigma_{nom} = pD/(2t) \tag{2}$$

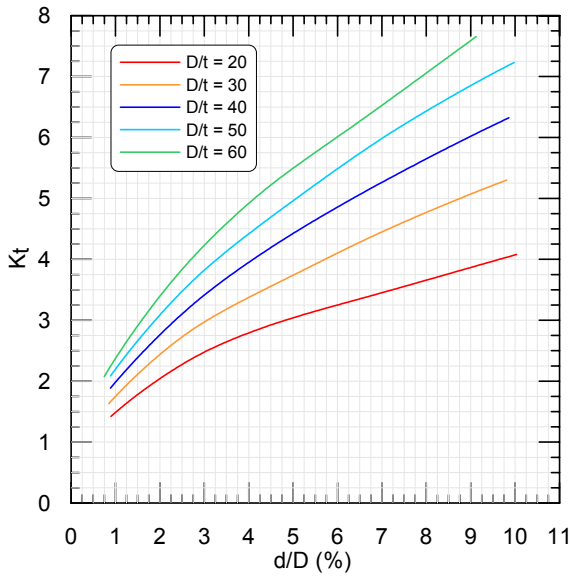

Figure 12. K_t versus d/D ratio for X60 steel pipes, being d the depth after removal of the indenter.

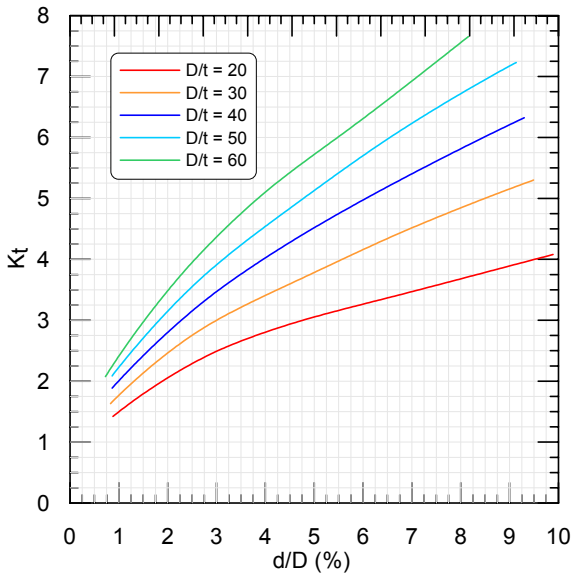

Figure 13. K_t versus d/D ratio for X60 steel pipes, being d the depth after re-rounding at zero pressure.

Each model geometry was submitted to fives analyses, in which different indentation depths were considered. Stress concentration factors were obtained from the last two steps (after re-rounding), when the dented region deforms elastically. The graphs of Figs. 12 and 13 show the results of stress concentration factors (K_t) versus d/D ratio for different D/t ratios of dented X60 line pipes. The difference between them is the depth of the dent (d) considered. In Fig 12 d is the depth after removal of the indenter, while in Fig. 13 d is the depth after re-rounding at zero pressure. For instance, a d/D ratio of 8% gives K_t approximately equal to 7.0 and 7.5 for a D/t ratio of 60 in the graphs of Figs. 12 and 13, respectively. For practical applications, the graph of Fig. 13 seems to be more plausible, since field mapping of damaged pipes presumes that internal pressure may have caused an amount of re-rounding at the dented region.

The definition of the theoretical stress concentration factor, presented in Eq. (1), applies mainly to ideal elastic materials and depends on the geometry of the body and the loading. However, in the analyzed case a more realistic

model is necessary, since the level of the applied loads implies in plastic deformations. For this case, it is considered the concept of the effective stress concentration factor (K_e), Pilkey, 1997. This factor depends on the characteristics of the material and the nature of the load, as well as the geometry of the stress raiser. The magnitude of K_e is obtained experimentally. Also, it can be noted that $1 \leq K_e \leq K_t$. To express the relationship between K_e and K_t the concept of notch sensitivity (q) is introduced (Pilkey, 1997):

$$K_e = q(K_t - 1) + 1 \tag{3}$$

For fatigue loading, K_e must be replaced by the fatigue notch factor (K_f), defined as

$$K_f = \sigma_f / \sigma_{nf} \tag{4}$$

where σ_f and σ_{nf} are the fatigue limit of unnotched and notched specimens, respectively. The Eq. (3) can be rewritten replacing K_e by K_f. For the correct determination of the q value, it is necessary fatigue tests to be carried out. It will be made in the next phase of this work.

6. Concluding remarks

A finite element model to estimate stress concentration factors in dented pipes under cyclic internal pressure was developed. The numerical procedure was calibrated with the aid of experimental tests using small-scale pipe models. The experiments reproduced the strain history at the damaged region during indentation and pressurization. In view of the good correlation obtained between the numerical and experimental results, the FE model was used to generate SCFs of dented X60 pipes under cyclic internal pressure.

The experiments showed that dented steel pipes under cyclic internal pressure may be considered to deform elastically if the maximum internal pressure is not increased. The dented region of the pipe re-rounds after the first cycle of pressure but no further plastic strain will occur if the internal pressure is lower than a previously applied maximum value. It shows that perhaps the SCF may be obtained from a simple linear elastic analysis if the dented geometry is reproduced as an initial configuration of the FE mesh. In this case, the effect of residual stresses would be ignored. This approach will be investigated in a future work.

The model will also be used to carry out a parametric study for different types of initial dents and materials. If the effect of the residual stresses is substantial, the strain hardening of the material will influence the SCFs. Also, there is a difference when the SCF is estimated from the hoop stress, the von Mises stress or the stress intensity factor (Alexander and Kiefner, 1997). Finally, for the estimation of fatigue in dented pipes under internal cyclic pressure the parameter q of Eq. (5) must be appropriately determined. Ideally, this is done experimentally, in this case by means of fatigue tests of dented pipe specimens.

7. Acknowledgements

The authors would like to acknowledge the technician Marcos Tadeu A. Dias and the financial support from PETROBRAS and National Petroleum Agency (ANP) at different stages of this research work.

8. References

ABAQUS, 2004, “User’s and Theory Manuals”, Release 6.4, Hibbitt, Karlsson, Sorensen, Inc.

Alexander, C.R., Kiefner, J.F., 1997, “Effects of Smooth and Rock Dents on Liquid Petroleum Pipelines”, Final Report to The American Petroleum Institute, Stress Engineering Services, Inc. and Kiefner and Associates, Inc., API Publication 1156.

Cosham, A., Hopkins, P., 2004, “The Effect of Dents in Pipelines—Guidance in the Pipeline Defect Assessment Manual”, International Journal of Pressure Vessels and Piping, Vol. 81, No. 2, pp. 127-139.

Fowler, J.R., 1993, “Criteria for Dent Acceptability in Offshore Pipeline”, Proceedings of the 25th Offshore Technology Conference, OTC 7311, Houston, USA, pp 481-493.

Pilkey, W.D., 1997, “Peterson’s Stress Concentration Factors”, Ed. Wiley-lnterscience, United States of America, 524 p.

9. Responsibility notice

The authors are the only responsible for the printed material included in this paper.